ACS APPLIED ENERGY MATERIALS
Cite This: ACS Appl. Energy Mater. 2018, 1, 4075−4083
Article
www.acsaem.org

Copper Selenides as High-Efficiency Electrocatalysts for Oxygen Evolution Reaction

Jahangir Masud, Wipula P. R. Liyanage, Xi Cao, Apurv Saxena, and Manashi Nath*

Department of Chemistry, Missouri University of Science & Technology, Rolla, Missouri 65409, United States

Supporting Information

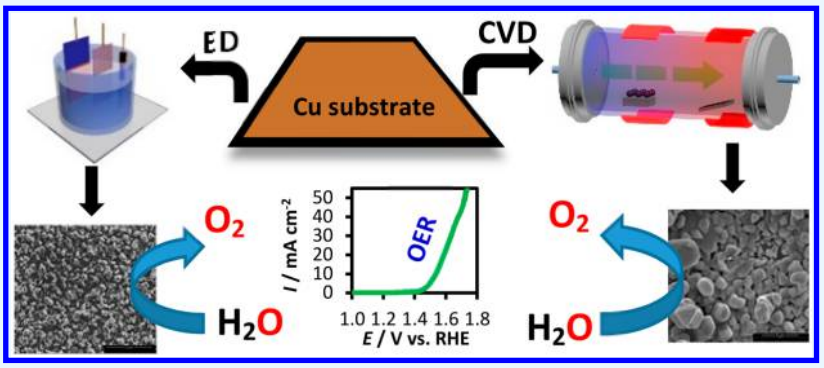

ABSTRACT: Designing high-efficiency water oxidation catalysts from earth-abundant resources has attracted significant attention in the last couple of years owing to the potential application of this technology in several energy conversion devices. Among the transition metals, copper is one of the cheapest earth-abundant nonprecious element which can enhance electrocatalytic activity due to heavily occupied *d*-orbitals. In this article we have shown electrocatalytic activity of copper selenide for the first time for water oxidation reaction. The copper selenide phases were synthesized by direct electrodeposition on electrodes, as well as by hydrothermal and chemical vapor deposition (CVD) techniques. Structure and morphology characterization through powder X-ray diffraction, Raman, X-photoelectron spectroscopy, and electron microscopy revealed that all the synthesized phases were pure crystalline copper selenide of composition Cu_2Se and comprising nanostructured granular morphology. Electrocatalytic performance for water oxidation was investigated in alkaline solution (1 M KOH) and it was observed that Cu_2Se showed a low overpotential of only 270 mV to achieve 10 mA cm^{-2}. This catalyst also displayed a low Tafel slope of 48.1 mV dec^{-1}. Interestingly Cu_2Se showed comparable electrocatalytic activity irrespective of the method of synthesis indicating that it is indeed an intrinsic property of the material. Chronoamperometric studies revealed that the catalyst retained its activity for prolonged periods of continuous oxygen evolution exceeded 6 h, while postactivity characterization revealed that crystallinity and surface composition was preserved after catalytic activity. Because copper selenides can be found in nature as stable minerals, this article can initiate a new concept for efficient catalyst design.

KEYWORDS: *OER, copper selenides, water splitting, CVD, transition metal chalcogenides*

1. INTRODUCTION

Electrochemical oxygen evolution reaction (OER) representing the challenging anodic half-cell reaction in both H_2 evolution through water splitting and conversion of CO_2 to fuel, has received considerable and persistent attention over the last several decades.[1−4] Water splitting and CO_2 electroreduction are considered as two of the most promising techniques for sustainable generation of renewable fuels. However, the kinetically sluggish $4e^-$ oxidation process in OER ($4OH^- \rightarrow O_2 + 2H_2O + 4e^-$) requires high energy and is the most challenging aspect for large-scale deployment of these energy conversion processes.[5−8] One approach to address this problem is the development of efficient catalysts for OER. Although iridium dioxide (IrO_2)[9] and ruthenium dioxide (RuO_2)[10] have been known as state-of-the-art OER electrocatalysts with low overpotential, their high cost and scarcity of elements makes these catalysts unsuitable for economically feasible hydrogen production in a practically usable scale.

Recently, much effort has been devoted to improve the OER electrocatalytic activity by exploring noble-metal free electrocatalysts.[11−17] Indeed, a variety of non-noble metal-based compounds with attractive catalytic efficiency and stability have been explored in recent years. Particularly, earth abundant transition metals comprising Ni, Fe, Co, and their oxides were widely studied as OER catalysts in alkaline media.[13,17] Among these, the transition metal chalcogenides (M_xE_y, M = Ni, Fe, Co and E = S, Se) have gained considerable attention due to their exceptional electrocatalytic activity toward OER, ORR (oxygen reduction reaction), and HER (hydrogen evolution

Received: May 10, 2018
Accepted: July 26, 2018
Published: July 26, 2018

DOI: 10.1021/acsaem.8b00746
ACS Appl. Energy Mater. 2018, 1, 4075−4083

reation) in alkaline media.[18−25] Research from several groups including our own have shown high catalytic activity for Ni-chalcogenides such as NiSe,[18] Ni_3Se_2,[20] $NiSe_2$,[22] Ni_3S_2,[26] Ni_3Te_2,[27] cobalt selenides, Co_7Se_8,[19,28] and $CoSe_2$,[29] for OER, HER, and ORR. However, apart from enhanced performance, reducing the electrocatalyst cost without compromising performance has still been the focus of further research and tremendous efforts have been devoted by many researchers in that direction. One of the easiest way to reduce the cost is to design the catalyst from the most earth abundant and cheap elements.

Copper is widely available in the earth's crust and cheaper than most metals including Ir, Ni, Co, etc. Copper and its oxides can be easily synthesized via electrodeposition and hydrothermal methods. Despite the lower price and earth-abundancy, copper is rarely used as a water splitting catalyst due to the poor catalytic activity. Yang et al.[30] had synthesized Cu_2O/CuO bilayered composites by electrodeposition and subsequent thermal reduction and showed the high photochemical HER activity and stability. In another report, OER activity of $Cu(OH)_2$ based nanowire grown on Cu foil[31] was reported, where 530 mV overpotential was required to achieve the current density of 10 mA cm^{-2}. Unfortunately, the high overpotential renders it economically unsuitable as a replacement for Ir. Previously we have observed that the catalyst activity in the transition metal based electrocatalysts can be enhanced by increasing covalency in the metal−anion bond.[27] Hereby, we propose that Cu-based chalcogenides will show better electrocatalytic activity compared to the oxides since covalency increases down the chalcogenide series away from oxygen.

In this work we have reported the highly efficient electrocatalytic activity of copper selenide (Cu_2Se) nanostructures obtained via different synthesis routes, such as electrodeposition, hydrothermal method, and chemical vapor deposition. These simple binary copper selenides show improved oxygen evolution with high efficiency in alkaline medium and exhibit high stability for prolonged period of time. The overpotential (η) at a current density of 10 mA cm^{-2} was obtained at 270 mV, which was significantly lower than the oxide-based catalysts including state-of-the-art RuO_2 and IrO_2 and is among the lowest overpotentials observed till date. The low Tafel slopes (48.1 mV dec^{-1}) also indicate better OER kinetics for these copper selenide electrocatalyst. It should be also noted that there are very few reports of binary copper compounds as OER electrocatalyst with Cu being the catalytically active site. Additionally, this is one of the first reports of OER catalytic activity in the family of binary copper chalcogenides.

2. EXPERIMENTAL SECTION

Materials. All the chemicals used for the synthesis were of analytical grade and were used without further purification. All solutions were prepared using deionized water (DI: resistivity 18 MΩ cm). Copper sulfate ($CuSO_4$) was purchased from Fisher Scientific, Selenium dioxide (SeO_2) and hydrazine hydrate ($N_2H_4{\cdot}H_2O$, 100%) were purchased from the Acros Organics. Au coated glass slides (Au-glass, hereafter) were bought from Deposition Research Lab Incorporated (DRLI) Lebanon, Missouri.

Electrodeposition of Copper Selenide (Cu_2Se). Conventional three-electrode system was used for the electrodeposition of copper selenide films on different conducting substrates (e.g., Cu, Au-glass, glassy carbon (GC), etc.). AglAgCl and GC plate were used as the reference and counter electrode, respectively. Substrates were cleaned by micro-90 detergent followed by sonication in mixture of isopropanol, ethanol, and deionized water. The clean and air-dried substrates were masked with a scotch tape, leaving a circular exposed geometric area of known dimensions (0.08 cm^2) for the electrodeposition. Electrodeposition of copper selenide films were carried out from an electrolytic bath containing 10 mM $CuSO_4$, 10 mM SeO_2, and 25 mM LiCl at 25 °C. Dilute HCl was added to adjust the pH at 2.4. Before electrodeposition, N_2 gas was purged through the solution for 30 min to remove all dissolved O_2 from the elcetrochemical bath. Electrodeposition was carried out for 300 s at −0.7 and −0.8 V (vs AglAgCl). After deposition the films were thoroughly washed with DI water to remove any adsorbents from the surface of the film.

Hydrothermal Synthesis of Copper Selenide (Cu_2Se). In a typical synthesis, Cu_2O (1.0 mM) was dissolved in 5.0 mL of deionized water under magnetic stirring to form a homogeneous solution. After mixing the solution for 10 min, Se powder (1.0 mM) was added and stirred vigorously for 20 min. Finally, $N_2H_4{\cdot}H_2O$ (2.0 mL) was added to the mixture and stirred continuously for another 10 min. The resulting solution was transferred to a Teflon-lined stainless-steel autoclave. The autoclave was sealed and maintained at 185 °C for 24 h, then naturally cooled to room temperature. The black product formed was centrifuged, washed several times with DI water, and then with mixture of ethanol and DI water to remove impurities. The product was dried in a vacuum oven at 25 °C for 12 h.

Chemical Vapor Deposition (CVD) of Copper Selenide (Cu_2Se). Cu_2Se sample synthesis by a chemical vapor deposition (CVD) technique was carried out in a horizontal tube furnace at 700 °C under a constant flow of N_2 as carrier gas. The flow rate of N_2 was maintained throughout the reaction at 120 sccm with the help of mass flow controllers. Growth was carried out using Cu coated Si wafer cut into 1 cm × 2 cm pieces as the substrate and typically substrates were placed at the middle region of the furnace at 700 °C. Since Se sublimes at elevated temperatures, the Se shots were kept near the inlet of the reaction tube such that the temperature of selenium exceeds the sublimation temperature when the central zone of the furnace reaches 700 °C. Initially, Se (0.5 g of selenium shots) was kept outside of the heating zone by pushing the ceramic liner of the furnace to the extreme left. Once the central zone of the furnace reached 700 °C, the ceramic liner was pushed to the right such that the Se shots were in the 400 °C zone. This is a crucial step for the reproducibility of the reaction as this step prevents the escape of Se before the growth zone at the center of the furnace reaches the intended reaction temperature (700 °C). The reaction was carried out for 30 min, and the furnace was cooled down to room temperature at a rate of 8 °C min^{-1}. As prepared samples were further annealed at 140 °C for 60 min under nitrogen atmosphere before further characterization.

Electrode Preparation. The electrodeposited and CVD synthesized samples were prepared directly on the electrode which were used as-synthesized for electrochemical measurements. To analyze the activity of hydrothermally synthesized Cu_2Se, a homogeneous catalyst ink was prepared by adding 5.0 mg of catalyst powder in 250.0 μL of Nafion solution (50 μL of 1% nafion solution in 50 μL of 50% IPA in water) followed by ultrasonication for 30 min. 20 μL of the ink dispersion was drop casted on a confined area (0.08 cm^2) on Cu substrate. The drop-casted film was then dried at room temperature and finally heated at 130 °C for 30 min in an oven.

In this article, we have reported copper selenide (Cu_2Se) catalyst by using different synthetic routes and hereafter electrochemically deposited catalysts will be denoted as Cu_2Se (ED-1) and Cu_2Se (ED-2) for the deposition potential at −0.8 and −0.7 V vs AglAgCl, respectively, hydrothermally synthesized catalyst as Cu_2Se (HD), and chemical vapor deposited catalyst as Cu_2Se (CVD).

3. RESULTS AND DISCUSSION

Structural and Morphological Characterization. The variation of phase compositions of copper selenide synthesized by different methods were investigated by powder X-ray diffraction (pxrd). Figure 1a shows the crystalline pxrd patterns

DOI: 10.1021/acsaem.8b00746
ACS Appl. Energy Mater. 2018, 1, 4075−4083

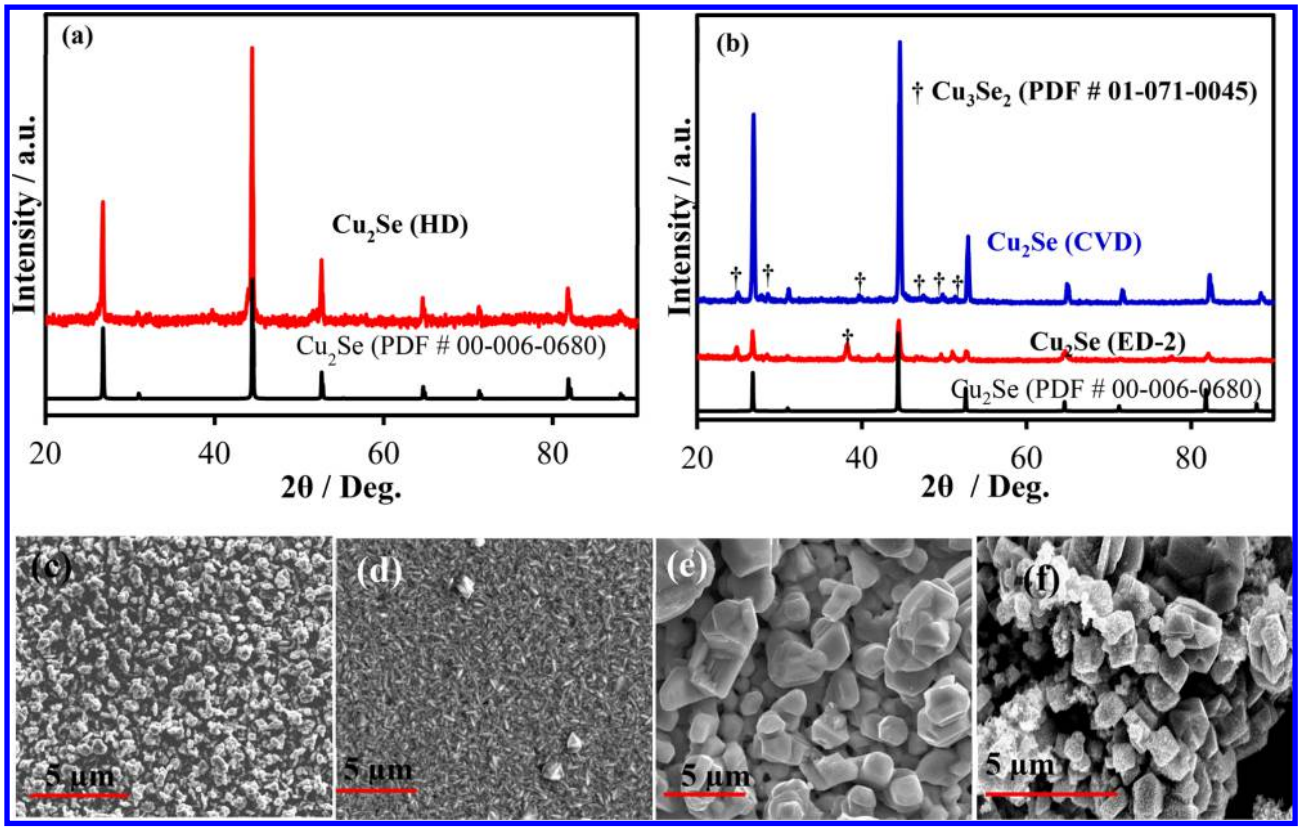

Figure 1. PXRD patterns of (a) hydrothermally synthesized Cu_2Se and (b) CVD (blue) and electrodeposited (red) Cu_2Se catalysts along with the corresponding reference spectra. SEM images of (c) electrodeposited Cu_2Se (ED-1 at −0.8 V)), (d) electrodeposited Cu_2Se (ED-2 at −0.7 V), (e) chemical vapor deposited Cu_2Se (CVD), and (f) hydrothermally synthesized Cu_2Se (HD) catalysts.

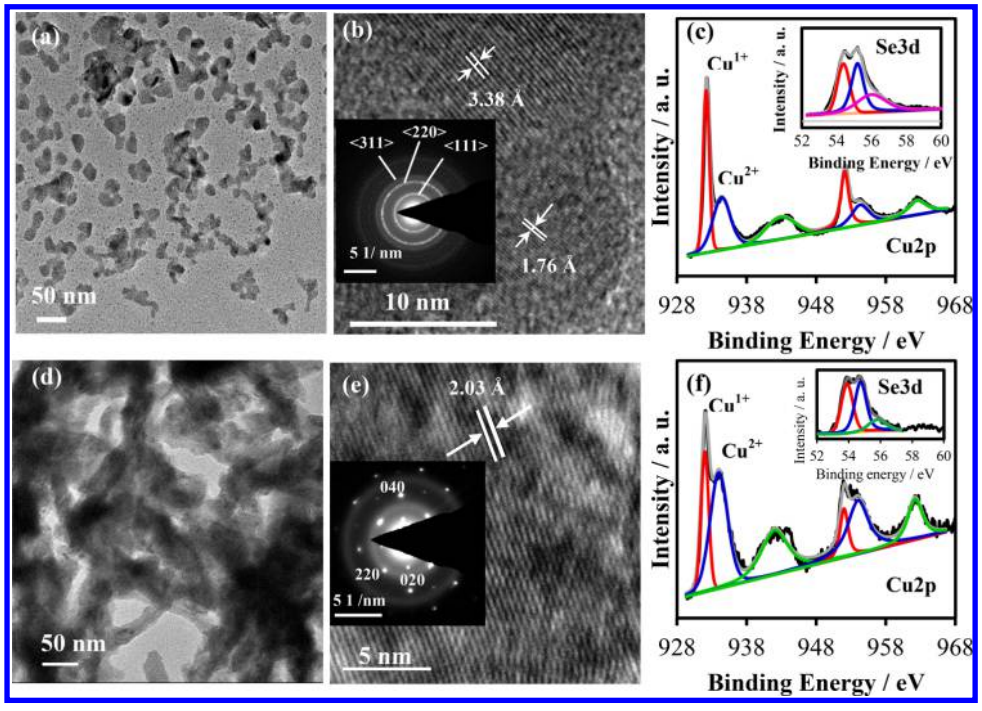

Figure 2. TEM images of (a and b) Cu_2Se (ED-1) and (d and e) Cu_2Se (CVD). (b and e, insets) SAED of Cu_2Se (ED-1) and Cu_2Se (CVD), respectively. (c and f) XPS of Cu 2p of Cu_2Se (ED-1) and Cu_2Se (CVD), respectively. (c and f, insets) Corresponding Se 3d spectra.

of hydrothermally synthesized pure copper selenide which is nicely consistent with the standard diffraction pattern for Cu_2Se (PDF no. 00-006-0680). The electrochemically deposited Cu_2Se(ED-1) (deposited at −0.8 V vs Ag|AgCl) on the other hand, showed a lesser degree of crystallinity as shown in supporting Figure S1. It has been reported previously that electrodeposition frequently produces poorly crystalline or even amorphous films. The crystallinity of the electrodeposited

DOI: 10.1021/acsaem.8b00746
ACS Appl. Energy Mater. 2018, 1, 4075−4083

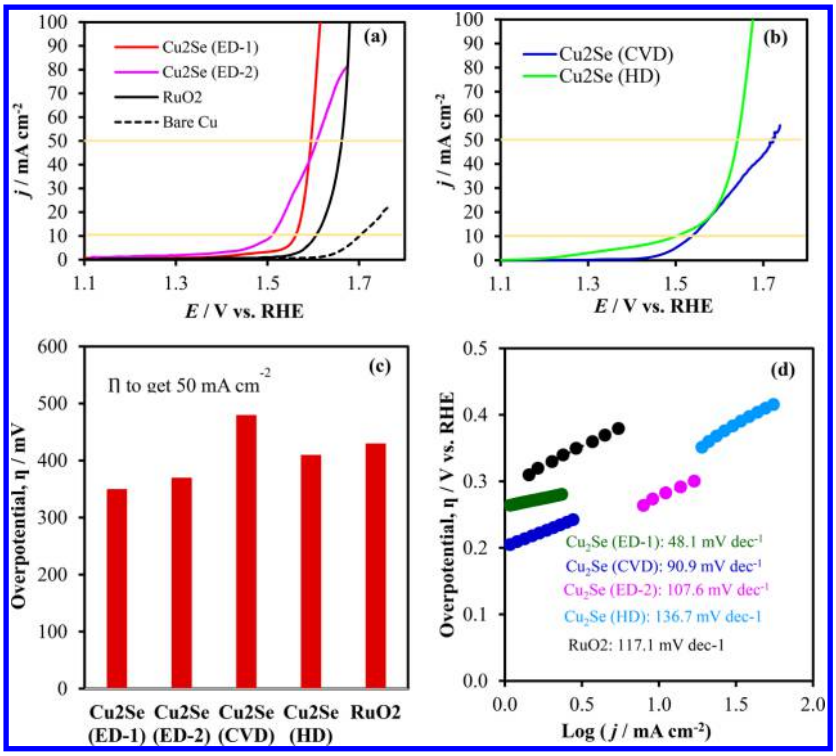

Figure 3. OER polarization curves (a and b) in N_2 saturated 1 M KOH solution for different catalysts. (c) OER overpotential, η to achieve 50 mA cm^{-2} at different catalysts, and (d) Tafel plots of catalysts.

films was greatly affected by the change of deposition potential in the same electrochemical bath. Crystalline Cu_2Se (PDF no. 00-06-0680) was obtained at a deposition potential of −0.7 V (vs AglAgCl) with some Cu_3Se_2 (PDF no. 01-071-0045) present as a minor impurity phase. For CVD synthesis, the pattern also showed mainly Cu_2Se phase with minor presence of Cu_3Se_2 as shown in Figure 1b. The closeness of the pxrd patterns with the Cu_2Se and Cu_3Se_2 confirmed that copper selenide was a major product for all of these synthesis procedures. The morphology of as prepared copper selenide films were studied by SEM. Figure 1c−f show SEM images of Cu_2Se (ED-1), Cu_2Se (ED-2), Cu_2Se (CVD), and Cu_2Se (HD), respectively. It was revealed that the electrodeposited films (Figure 1c and d) are relatively uniform, well-dispersed, and composed of randomly oriented nanoparticles. This type of morphology may lead to a very rough surface with high porosity which is beneficial for enhanced catalytic activity. The CVD, Cu_2Se film, and hydrothermally synthesized Cu_2Se powder showed different morphologies as can be seen in Figure 1e and f. These are mainly granular with size distribution of nanometer to few micrometers. The chemical compositions of these films, as analyzed by EDS, are shown in supporting Figure S2a−d. The EDS confirms the presence of Cu and Se in the all samples and absence of even trace amount of oxygen. The atomic ratio of Cu:Se was calculated as approximately 2.0:1.0, 2.0:1.0, 1.9:1.0, and 2.0:1.0 for Cu_2Se (ED-1), Cu_2Se (CVD), Cu_2Se (ED-2), and Cu_2Se (HD), respectively, which also confirmed that the major phase was Cu_2Se in all these samples. The EDS measurements were performed at several locations on the sample surface to confirm uniform chemical compositions.

Transmission electron microscopy (TEM) images of the representative Cu_2Se (ED-1) and Cu_2Se (CVD) catalyst has been shown in Figure 2a and d, respectively. It can be seen (Figure 2a) that the Cu_2Se (ED-1) are nanoparticles with smooth surfaces have relatively symmetrical shapes with size in the range of 20−40 nm. On the other hand, chemical vapor deposited Cu_2Se (CVD) shows interconnected nanoparticles (Figure 2d). HRTEM image of Cu_2Se (ED-1) showed multiple lattice fringes as shown in Figure 2b with measured *d*-spacings of 3.38, 1.76 Å corresponding to the (111) and (311) planes of Cu_2Se, respectively. Lattice fringes correspond to (220) plane (spacing of 2.03 Å) could be easily indexed from HRTEM of Cu_2Se (CVD) catalyst (Figure 2e). In addition, the crystallinity of catalysts was further confirmed by selected area electron diffraction (SAED) patterns. A characteristic SAED pattern of Cu_2Se (ED-1) (inset of Figure 2b) was indexed to the (111), (220), and (311) planes while the SAED pattern for Cu_2Se (CVD) showed spots corresponding to (020), (220), and (040) reflections of Cu_2Se, thereby corroborating the indexed HRTEM (inset of Figure 2e).

The oxidation state of the elements in copper selenide samples were investigated by X-ray photoelectron spectroscopy (XPS). Figure 2c represents the deconvoluted Cu 2p XPS peak for Cu_2Se (ED-1) catalyst where the strong fitting of peaks at 932.2 and 952.2 eV for Cu^{1+} $2p_{3/2}$ and $2p_{1/2}$ peaks and 934.2 and 954.3 eV for Cu^{2+} $2p_{3/2}$ and $2p_{1/2}$ peaks, respectively confirmed the presence of Cu in +1/+2 mixed oxidation states. Obvious satellite peaks were observed at 943.2 and 962.4 eV possibly due to the overlapping of antibonding orbital between the Cu and Se. Similar oxidation states of Cu could be assigned for Cu_2Se (CVD) catalyst as shown in Figure 2f where peaks at 932.1 and 952.2 eV for Cu^{1+} $2p_{3/2}$ and $2p_{1/2}$ peaks and binding energies at 934.2 and 954.4 eV for Cu^{2+} $2p_{3/2}$ and $2p_{1/2}$ peaks. These binding energy values nicely matched with previous report of Cu_2Se.[32−34] It should be mentioned that Cu at the surface of both electrodeposited and CVD synthesized Cu_2Se showed mixed oxidation states of +1 and +2. The coexistence

DOI: 10.1021/acsaem.8b00746
ACS Appl. Energy Mater. 2018, 1, 4075−4083

of +1 and +2 mixed valence is well-known in Cu_2Se.[32] The deconvoluted Se 3d XPS spectra of electrodeposited Cu_2Se (inset of Figure 2c) and chemically vapor deposited Cu_2Se (inset of Figure 2f) catalysts showed peaks at 54.1 and 55.0 eV for the Se $3d_{5/2}$ and Se $3d_{3/2}$, respectively, in accordance with previously reported for Cu_2Se.[34] The weaker shoulder peaks in Se 3d at 56.5 eV may result from the oxidation of Se^{2-} ions on the surface of the catalyst.[34] The Cu to Se atomic ratio of ~2.0:1.0 was calculated from the initial Cu $2p_{3/2}$ and Se $3d_{5/2}$ peak areas, demonstrating that the catalyst composition was indeed Cu_2Se. Hydrothermally synthesized pure Cu_2Se also exhibited similar XPS spectra as shown in Supporting Information Figure S3 confirming the presence of mixed valent Cu coordinated to Se^{2-}.

The Raman shift of Cu_2Se (ED-1) and Cu_2Se (CVD) is shown in Figure S4. The only intense peak, observed at 260 cm^{-1}, can be assigned to the Se−Se stretch vibration in Se^{2-} and is in good agreement with the value previously reported for Cu_2Se.[35] The absence of peaks at 141 and 235 cm^{-1} confirm that the film contains no elemental Se. It has also been noted that there is no evidence of oxidic phases as there is no substantial peak observed at about 500 cm^{-1}, characteristic of the oxide phase.

The electrocatalytic OER activity of Cu_2Se catalyst was investigated in 1 M KOH solution. A typical three electrode system electrochemical cell was used in this study where Cu_2Se modified Cu and/or GC substrate served as working electrode, KCl saturated AglAgCl as reference, and glassy carbon (GC) plate as counter electrodes. The reference AglAgCl electrode was calibrated using open circuit potential (OCP, −0.199 V) with a Pt wire in H_2-saturated H_2SO_4 solution and converted to a reversible hydrogen electrode (RHE) using the following equation, eq 1:

$$E_{RHE} = E_{AglAgCl} + 0.059pH + E^{\circ}_{AglAgCl} \quad (1)$$

where E_{RHE} is the converted potential vs RHE, $E_{AglAgCl}$ is the experimentally obtained potential vs AglAgCl reference electrode, and $E^{\circ}_{AglAgCl}$ is the standard potential of AglAgCl (0.199 V).

The linear sweep voltammetry (LSV) was performed in N_2-saturated 1 M KOH solution at a scan rate of 10 mV s^{-1}. Figure 3a and b shows the OER polarization curves recorded for different catalysts. It can be seen that Cu itself exhibits poor OER activity in alkaline medium. However, the simple modification of Cu substrates by chemical vapor deposition, hydrothermally synthesized, and/or electrodeposition of copper selenide demonstrates exceptionally high OER activity. The OER onset potentials for Cu_2Se (CVD), Cu_2Se (ED-2), Cu_2Se (HD), and Cu_2Se (ED-1) were obtained as 1.45, 1.45, 1.50, and 1.53 V vs RHE, respectively. Surprisingly, both electrochemically (ED-2) and chemical vapor deposited Cu_2Se catalyst show similar onset potentials which confirms the intrinsic properties of catalyst which is independent of synthesis history and surface morphology.

The slower rise in oxidation current density for the hydrothermally synthesized sample compared to the electrodeposited one can be attributed to the fact that while the electrodeposited Cu_2Se grew directly on the electrode and produced a binder-free film, the hydrothermally synthesized sample was assembled on the electrode with the help of Nafion, which limited exposure of the active sites as well as introduced contact resistance between the catalyst and electrode. Such reduction in activity between the hydrothermally synthesized and electrodeposited catalyst has also been observed for other OER electrocatalysts.[27] The efficiency of OER catalysts were obtained by measuring the overpotential (η) required to get the geometric current density of 10 mA cm^{-2} which is believed to be equivalent of 10% solar energy conversion efficiency.[35] It was found that the current density of 10 mA cm^{-2} was almost unreachable for the bare Cu electrode over the span of applied potential range. On the other hand, only 270, 290, 300, and 320 mV overpotentials were needed to achieve the current density of 10 mA cm^{-2} for Cu_2Se (ED-2), Cu_2Se (HD), Cu_2Se (CVD), and Cu_2Se (ED-1), respectively. The lower overpotential (by ~30 mV) in electrochemically synthesized Cu_2Se (ED-2) catalyst compared to CVD catalyst implies that the surface morphology and nanostructuring also plays a vital role in OER activity. Along with that the coexistence of Cu_3Se_2 as a minor phase in the Cu_2Se (CVD) and Cu_2Se (ED) may also play synergistic role in the enhancing the catalytic activity. The effect of surface morphology, substrate effect as well as growth conditions can also be seen when comparing the overpotential at higher current densities (50 mA cm^{-2}) as shown in Figure 3c. Interestingly the lowest overpotentials were required for the electrodeposited samples, Cu_2Se (ED-1) and Cu_2Se (ED-2) catalysts. The rationale for this observation might be attributed to the highly porous morphology and smaller nanoparticles in the catalytic film compared to other copper selenide catalysts, as well as the advantages of direct electrodeposition of the catalyst which produces a binder-free catalytic film with direct electrical contact with the electrode and containing no nonactive components thereby maximizing charge transport and catalytic efficiency. The hydrothermally synthesized sample on the other hand was attached to the electrode with the help of Nafion, which reduces the exposure of the active sites to the electrolyte as well as inhibits charge transport. The difference observed in catalytic activity between samples produced from different synthetic routes can also be attributed to the difference in particle/grain size apart from the direct adherence of the film to the electrode as well as surface morphology. It is also possible that degree of crystallinity of the catalytic film plays an influential role on its activity. While Cu_2Se(ED-1) showing best catalytic activity was amorphous, the other films were crystalline. Generally, amorphous films show better catalytic activity due to more exposure of the active sites to the electrolyte. Apart from this, the onset potential as well as Tafel slopes of Cu_2Se (ED-2), Cu_2Se (HD), and Cu_2Se (CVD) were almost similar. The catalytic performance was also normalized with respect to catalyst loading as shown in Figure S5. It was observed that the electrodeposited samples showed the best gravimetric current density at a fixed overpotential compared to the CVD-grown and hydrothermally synthesized samples, respectively. This observation further confirms that the electrodeposited sample owing to its direct attachment to the electrode, smaller grain size, and lower degree of crystallinity, exhibits enhanced catalytic performance even with low loading. Note that the OER activity of the copper selenide nanostructures was better than state-of the-art of RuO_2 as well as other reported CuO based catalyst.[31,36,37] The greatly improved electrocatalytic OER activity of Cu_2Se (ED-1) compared to CuO can be ascribed to the effect of lower electronegativity of Se vs O leading to increase in covalency of the Cu−Se bond. Similar observations have been reported previously for transition metal

DOI: 10.1021/acsaem.8b00746
ACS Appl. Energy Mater. 2018, 1, 4075−4083

Table 1. Comparison of OER Activities at Different Cu-Based Electrocatalysts

catalysts	electrolyte	onset potential/V vs RHE	η at 10 mA cm^{-2}/mV	catalyst loading/mg cm^{-2}	Tafel slopes/mV dec^{-1}	refs
$Cu(OH)_2$ NWS/CF	0.1 M NaOH	1.625	530	0.8	86	31
CuO NWS/CF	0.1 M NaOH	1.627	590	0.8	84	31
CuO_x NWS/CF	0.1 M NaOH	1.67	630	0.8	108	31
Annealed CuO	1.0 M KOH	1.58	430 (1 mA cm^{-2})		61.4	36
H_2O_2 treated CuO	0.1 M KOH	1.57	520 (2.5 mA cm^{-2})			37
$Cu_{0.3}Ir_{0.7}O_\delta$	0.1 M KOH		415		105	38
$CuCo_2O_4$−SSM	1.0 M KOH	1.55	400	0.2		39
$CuRhO_2$	1.0 M KOH	1.56	410	0.8		40
Cu_3P/CF	0.1 M KOH		412 (50 mA cm^{-2})	68.5	63	41
Cu_2Se (ED-1)	1.0 M KOH	1.53	320	0.8	48.1	this work
Cu_2Se (CVD)	1.0 M KOH	1.45	300	2.0	90.9	this work
Cu_2Se (ED-2)	1.0 M KOH	1.45	270	0.7	107.6	this work
Cu_2Se (HD)	1.0 M KOH	1.50	290	5.0	136.7	this work

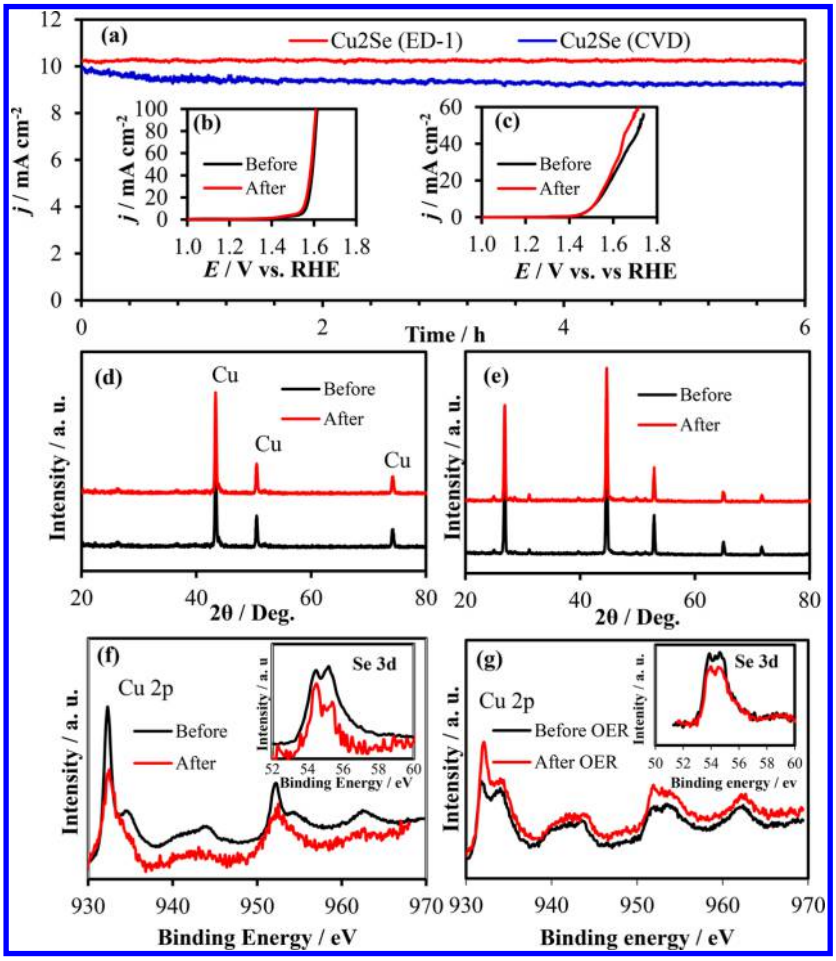

Figure 4. (a) OER stability in 1 M KOH solution at a constant potential of 1.55 V for Cu_2Se (ED-1) and 1.53 V vs. RHE for Cu_2Se (CVD). Comparison of LSVs of (b) Cu_2Se (ED-1) and (c) Cu_2Se (CVD) after chronoamperometry. XRD (d) and XPS (f) for Cu_2Se (ED-1) and XRD (e) and XPS (g) for Cu_2Se (CVD) after stability.

chalcogenides-based catalysts where more covalent metal-selenide bond enhanced catalytic activity of the binary and ternary selenides.[20−22,27] The OER activities of different Cu-based electrocatalyst are shown in Table 1.

The Tafel slope is an important factor for the evaluation of catalyst kinetics which describes the influence of potential, or overpotential on steady-state current density. To gain further insight into the OER activities of these catalysts, Tafel slopes, were retrieved from the LSVs and are presented in Figure 3d. A linear dependency of η vs log(j) was achieved for all copper selenide catalysts and slopes were presented in Table 1. The lowest Tafel slopes was obtained for Cu_2Se (ED-1) catalyst (48.1 mV dec^{-1}) indicating better OER kinetics, highlighting the effect of nanostructure of catalyst along with porous network. Impressively, the estimated Tafel slopes of Cu_2Se is lower than well studied RuO_2 (117.1 mV dec^{-1}) catalyst. The OER activity tested for RuO_2 in Figure 3 is in good agreement with recently reported results in literature and it further validate our electrochemical measurements.[42,43] Both electrochemically and chemical vapor deposited Cu_2Se (ED-2 and

DOI: 10.1021/acsaem.8b00746
ACS Appl. Energy Mater. 2018, 1, 4075−4083

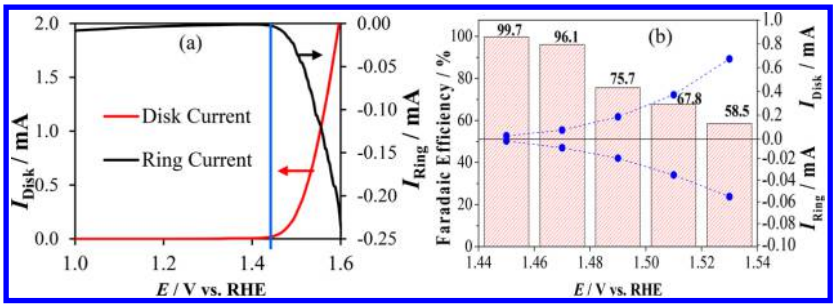

Figure 5. (a) Plots for the ORR−OER reaction showing OER current density at Cu_2Se (ED-1)/GC disk electrode in N_2-saturated 1.0 M KOH and ORR current density at Pt ring electrode maintained at 0.2 V vs RHE as a function of applied disk potential. The blue line indicates the onset potential for OER at the disk electrode corresponding with the onset of ORR at the ring electrode. (b) Faradaic efficiency of catalyst measured in N_2 saturated 1.0 M KOH at 1600 rpm rotation speed.

CVD) catalyst exhibited almost similar slopes which indicated that the reaction mechanism followed a similar pathway. The higher Tafel slope for hydrothermally synthesized Cu_2Se can be attributed as due to the effect of noncatalytic Nafion which was used to adhere the catalyst film on the electrode surface.

The stability of the Cu_2Se (ED-1) and Cu_2Se (CVD) electrocatalysts were investigated with chronoamperometric studies whereby, the catalytic film was maintained at a constant potential to generate oxygen in 1 M KOH solution for an extended period of time. The potential to achieve 10 mA cm^{-2} current density was selected for the chronoamperometric studies as shown in Figure 4a.

The potentials of 1.53 and 1.55 V vs RHE were chosen for the stability study and the electrolyte was continuously stirred at 1200 rpm to get rid of accumulated O_2 bubbles from the electrode surface.

It was observed that both catalysts (electrodeposited and CVD synthesized) showed exceptional stability of the OER catalytic activity in 1 M KOH and the current density did not show any degradation (Figure 4a). The comparison of LSVs before and after 6 h of oxygen generation were used to check the catalyst stability and has been shown in Figure 4b and c for electrodeposited Cu_2Se (ED-1) and Cu_2Se (CVD) catalyst, respectively. Interestingly, the LSV curves for both catalysts after OER did not show any noticeable decrease of onset potential and overpotential compared to the as-synthesized catalysts, and the LSVs before and after chronoamperometric studies were almost superimposable.

Composition of the catalysts following catalytic activity was investigated through pxrd, XPS, and SEM analyses. Figure 4d and e shows the comparison of pxrd patterns of Cu_2Se (ED-1) and Cu_2Se (CVD) catalyst, respectively after stability test. There was no change of pxrd patterns for both the samples after chronoamperometric studies. Structural and compositional integrity of both of the catalysts was further confirmed by XPS spectra of Cu 2p and Se 3d after OER activity and presented in Figure 4f and g. Surface morphology of the both catalyst checked through SEM imaging after activity did not reveal major changes in morphology (Figure S6) for both Cu_2Se (ED-1) and Cu_2Se (CVD) catalysts.

Testing of Evolved Gas and Faradaic Efficiency. A rotating ring disk electrode (RRDE) set up was used in bipotentiostat mode to monitor and quantify the gas evolved at the anode as shown in Figures 5 and S7. For this procedure Cu_2Se was electrodeposited on GC disk electrode in a RRDE setup and scanned at the anodic potential range while Pt ring was held a potential of 0.2 V (vs RHE). The idea was to hold the Pt ring potential suitable for ORR such that if any O_2 was being produced at the disk electrode, it will be collected and reduced at the ring electrode resulting in an increase of the ring current. Both the ring current and disk current were measured as a function of applied disk potential. Initially 1 M KOH solution was purged with N_2 gas for 30 min before starting the reaction to remove dissolved O_2 and blanketed in N_2 atmosphere. The disk electrode was scanned from 1.0 to 1.5 V (vs RHE) at a scan rate of 10 mV s^{-1} at 1600 rpm. Initially, the ring current was measured to be almost zero when disk current was almost zero. As soon as the disk current started to increase, the ring current also increased proportionately, indicating that there was indeed oxygen reduction happening at the Pt ring electrode and this O_2 was being generated at the disk electrode. Such an OER−ORR coupled reaction also leads to precise determination of the onset potential for OER. From Figure 5a the onset potential of OER was obtained as 1.44 V vs RHE. The OER faradaic efficiency of the catalyst was calculated from the ratio of ring and disk current and has been presented in Figure 5b. The highest Faradaic efficiency was obtained to be about 99.7% at the applied disk potential of 1.45 V (vs RHE) and decreased to 58.5% with the disk voltage increasing to 1.53 V (vs RHE).

Copper has been known as catalytically active center for several chemical conversion processes such as carbon dioxide reduction and hydrogenation catalysts.[44−50] Nevertheless, reports for electrocatalytic activity for Cu-based compounds toward water splitting is limited.[36−41] The presence of Cu^{2+} along with Cu^{1+} in this case is believed to be responsible for enhancement of OER catalytic activity by redistribution of electronic charge around the catalytic site through inductive effect of the neighboring metal atoms. In Cu_2Se, the bond between Cu^{1+} and Se^{2-} has a certain degree of polarization due to the electrostatic interactions between the anion and the cation. However, when Cu^{2+} ions are also present in the solid, the degree of covalency in the Cu−Se bonds can increase due to change in oxidation state of the metal (Cu^{2+} being more electronegative). Hence coexistence of Cu^{1+} and Cu^{2+} makes the anion−cation bonds nonidentical leading to inductive effects. Such inductive effect will lead to redistribution of electron density around the metal centers and can generate sites where OH group can bind more preferentially. Additionally, the heavily occupied *d*-orbitals along with the increased covalency in the Cu−Se bonds can be expected to push the occupied electronic states to be closer to the water oxidation level leading to lower overpotential and faster charge transfer across the catalyst(electrode)−electrolyte interference. Such an effect has recently been observed in the Ni-selenide and Ni-telluride series.[22,27] It is encouraging to observe such influence

DOI: 10.1021/acsaem.8b00746
ACS Appl. Energy Mater. 2018, 1, 4075−4083

of increased covalency on the OER catalytic activity in the Cu-based chalcogenides also. It must be mentioned here that copper selenides are found in nature as selenide minerals.[51] Cu_2Se in particular is known as berzelianite. Identifying such naturally occurring ores as stable and highly efficient water splitting electrocatalysts will lead to better catalyst design and have far-reaching implications for this energy conversion technology.

4. CONCLUSIONS

In summary, we have synthesized copper selenide nanostructure based electrocatalysts by electrodeposition, hydrothermal and CVD techniques and have comprehensively evaluated their catalytic activities for OER in alkaline conditions. The OER activity observed for all copper selenide samples which has been synthesized by different routes, suggests that the catalytic activity is indeed an intrinsic property of the material and independent of synthesis procedure. Electrodeposited Cu_2Se catalyst exhibits enhanced catalytic activity that could afford a current density of 10 mA cm^{-2} at a overpotential as low as 270 mV and with a low Tafel slope of 48.1 mV dec^{-1}. This catalyst shows excellent stability and structural integrity under continuous O_2 evolution condition for extended period of time (6 h). Cu being one of the cheapest and most earth-abundant elements available to mankind, this work makes an important contribution in identifying high-performance catalysts that can be used for practical applications in water splitting devices to produce sustainable and renewable energy for future needs.

■ ASSOCIATED CONTENT

Supporting Information

The Supporting Information is available free of charge on the ACS Publications website at DOI: 10.1021/acsaem.8b00746.

Characterization techniques, Faradaic efficiency, XRD of Cu_2Se (ED-1), SEM EDS of catalysts, XPS of Cu_2Se (HD), Raman spectra of ED-1, CVD, catalyst mass activity, SEM of ED-1 and CVD catalysts after stability, and OER−ORR experiment of Cu_2Se (ED-2) (PDF)

■ AUTHOR INFORMATION

Corresponding Author

*E-mail: nathm@mst.edu.

ORCID

Manashi Nath: 0000-0002-5058-5313

Notes

The authors declare no competing financial interest.

■ ACKNOWLEDGMENTS

The authors acknowledge financial support from the National Foundation (DMR 1710313), American Chemical Society Petroleum Research Fund (54793-ND10), and Energy Research and Development Center (ERDC) Missouri S & T. The authors would also like to acknowledge Materials Research Center for equipment use and Dr. Richard Brow for help with Raman measurements.

■ REFERENCES

(1) Kauffman, D. R.; Alfonso, D.; Tafen, D. N.; Lekse, J.; Wang, C.; Deng, X.; Lee, J.; Jang, H.; Lee, J.; Kumar, S.; Matranga, C. Electrocatalytic Oxygen Evolution with an Atomically Precise Nickel Catalyst. *ACS Catal.* **2016**, *6*, 1225−1234.

(2) Huan, T. N.; Rousse, G.; Zanna, S.; Lucas, I. T.; Xu, X.; Menguy, N.; Mougel, V.; Fontecave, M. A Dendritic Nanostructured Copper Oxide Electrocatalyst for the Oxygen Evolution Reaction. *Angew. Chem., Int. Ed.* **2017**, *56*, 4792−4796.

(3) Vermaas, D. A.; Smith, W. A. Synergistic Electrochemical CO_2 Reduction and Water Oxidation with a Bipolar Membrane. *ACS Energy Lett.* **2016**, *1*, 1143−1148.

(4) Han, L.; Tang, P.; Carmona, A. R.; Garcia, B. R.; Torrens, M.; Morante, J. R.; Arbiol, J.; Mascaros, J. R. G Enhanced Activity and Acid pH Stability of Prussian Blue-type Oxygen Evolution Electrocatalysts Processed by Chemical Etching. *J. Am. Chem. Soc.* **2016**, *138*, 16037−16045.

(5) Ma, W.; Ma, R.; Wang, C.; Liang, J.; Liu, X.; Zhou, K.; Sasaki, T. A Superlattice of Alternately Stacked Ni-Fe Hydroxide Nanosheets and Graphene for Efficient Splitting of Water. *ACS Nano* **2015**, *9*, 1977−1984.

(6) Hong, W. T.; Risch, M.; Stoerzinger, K. A.; Grimaud, A.; Suntivich, J.; Shao-Horn, Y. Toward the Rational Design of Non-Precious Transition Metal Oxides for Oxygen Electrocatalysis. *Energy Environ. Sci.* **2015**, *8*, 1404−1427.

(7) Lyu, F.; Bai, Y.; Li, Z.; Xu, W.; Wang, Q.; Mao, J.; Wang, L.; Zhang, X.; Yin, Y. Self-Templated Fabrication of CoO-MoO_2 Nanocages for Enhanced Oxygen Evolution. Adv. *Adv. Funct. Mater.* **2017**, *27*, 1702324.

(8) Chen, H.; Gao, Y.; Sun, L. Highly Active Three-Dimensional NiFe/Cu_2O Nanowires/Cu Foam Electrode for Water Oxidation. *ChemSusChem* **2017**, *10*, 1475−1481.

(9) Seitz, L. C.; Dickens, C. F.; Nishio, K.; Hikita, Y.; Montoya, J.; Doyle, A.; Kirk, C.; Vojvodic, A.; Hwang, H. Y.; Norskov, J. K.; Jaramillo, T. F. A highly active and stable IrO*x*/SrIrO3 catalyst for the oxygen evolution reaction. *Science* **2016**, *353*, 1011−1014.

(10) Lee, Y.; Suntivich, J.; May, K. J.; Perry, E. E.; Shao-Horn, Y. Synthesis and Activities of Rutile IrO_2 and RuO_2 Nanoparticles for Oxygen Evolution in Acid and Alkaline Solutions. *J. Phys. Chem. Lett.* **2012**, *3*, 399−404.

(11) Masud, J.; Umapathi, S.; Ashokaan, N.; Nath, M. Iron phosphide nanoparticles as an efficient electrocatalyst for the OER in alkaline solution. *J. Mater. Chem. A* **2016**, *4*, 9750−9754.

(12) De Silva, U. D.; Liyanage, W. P. R.; Nath, M. Magnetic Multifunctional Nanostructures as High-efficiency Catalysts for Oxygen Evolution Reactions. *MRS Advances* **2016**, *1*, 2401.

(13) Jiao, F.; Frei, H. Nanostructured Cobalt Oxide Clusters in Mesoporous Silica as Efficient Oxygen-Evolving Catalysts. *Angew. Chem., Int. Ed.* **2009**, *48*, 1841−1844.

(14) Amin, B. G.; Swesi, A. T.; Masud, J.; Nath, M. $CoNi_2Se_4$ as an efficient bifunctional electrocatalyst for overall water splitting. *Chem. Commun.* **2017**, *53*, 5412−5415.

(15) Tian, J.; Liu, Q.; Asiri, A. M.; Sun, X. Self-Supported Nanoporous Cobalt Phosphide Nanowire Arrays: An Efficient 3D Hydrogen-Evolving Cathode Over the Wide Range of pH 0−14. *J. Am. Chem. Soc.* **2014**, *136*, 7587−7590.

(16) Ledendecker, M.; Calderon, S. K.; Papp, C.; Steinruck, H. P.; Antonietti, M.; Shalom, M. The synthesis of nanostructured Ni_5P_4 films and their use as a non-noble bifunctional electrocatalyst for full water splitting. *Angew. Chem.* **2015**, *127*, 12538−12542.

(17) Peng, Z.; Jia, D.; Al-Enizi, A.; Elzatahry, A.; Zheng, G. From water oxidation to reduction: homologous Ni−Co based nanowires as complementary water splitting electrocatalysts. *Adv. Energy Mater.* **2015**, *5*, 1402031−1402038.

(18) Tang, C.; Cheng, N.; Pu, Z.; Xing, W.; Sun, X. NiSe Nanowire Film Supported on Nickel Foam: An Efficient and Stable 3D Bifunctional Electrode for Full Water Splitting. *Angew. Chem., Int. Ed.* **2015**, *54*, 9351−9355.

(19) Masud, J.; Swesi, A. T.; Liyanage, W. P. R.; Nath, M. Cobalt Selenide Nanostructures: An Efficient Bifunctional Catalyst with High Current Density at Low Coverage. *ACS Appl. Mater. Interfaces* **2016**, *8*, 17292−17302.

(20) Swesi, A. T.; Masud, J.; Nath, M. Nickel selenide as a high-efficiency catalyst for oxygen evolution reaction. *Energy Environ. Sci.* **2016**, *9*, 1771−1782.
(21) Masud, J.; Ioannou, P. C.; Levesanos, N.; Kyritsis, P.; Nath, M. A Molecular Ni-complex Containing Tetrahedral Nickel Selenide Core as Highly Efficient Electrocatalyst for Water Oxidation. *ChemSusChem* **2016**, *9*, 3128−3132.
(22) Swesi, A. T.; Masud, J.; Liyanage, W. P. R.; Umapathi, S.; Bohannan, E.; Medvedeva, J.; Nath, M. Textured $NiSe_2$ Film: Bifunctional Electrocatalyst for Full Water Splitting at Remarkably Low Overpotential with High Energy Efficiency. *Sci. Rep.* **2017**, *7*, 2401.
(23) Gao, M. R.; Cao, X.; Gao, Q.; Xu, Y. F.; Zheng, Y. R.; Jiang, J.; Yu, S. H. Nitrogen-doped graphene supported CoSe2 nanobelt composite catalyst for efficient water oxidation. *ACS Nano* **2014**, *8*, 3970−3978.
(24) Wang, C.; Jiang, J.; Ding, T.; Chen, G.; Xu, W.; Yang, Q. Monodisperse Ternary NiCoP Nanostructures as a Bifunctional Electrocatalyst for Both Hydrogen and Oxygen Evolution Reactions with Excellent Performance. *Adv. Mater. Interfaces* **2016**, *3*, 1500454.
(25) Zhang, J. J.; Su, H.; Wang, H. H.; Xue, Z. H.; Zhang, B.; Wei, X.; Li, X.; Hirano, S. I.; Chen, J. S. Constructing Ohmic contact in cobalt selenide/Ti dyadic electrode: The third aspect to promote the oxygen evolution reaction. *Nano Energy* **2017**, *39*, 321−327.
(26) Wu, Y.; Li, G. D.; Liu, Y.; Yang, L.; Lian, X.; Asefa, T.; Zou, X. Overall Water Splitting Catalyzed Efficiently by an Ultrathin Nanosheet-Built, Hollow Ni_3S_2-Based Electrocatalyst. Adv. *Adv. Funct. Mater.* **2016**, *26*, 4839−4847.
(27) De Silva, U.; Masud, J.; Zhang, N.; Hong, Y.; Liyanage, W. P. R.; Zaeem, M. A.; Nath, M. Nickel telluride as a bifunctional electrocatalyst for efficient water splitting in alkaline medium. *J. Mater. Chem. A* **2018**, *6*, 7608−7622.
(28) Masud, J.; Nath, M. Co_7Se_8 Nanostructures as Catalysts for Oxygen Reduction Reaction with High Methanol Tolerance. *ACS Energy Lett.* **2016**, *1*, 27−31.
(29) Kwak, I. H.; Im, H. S.; Jang, D. M.; Kim, Y. W.; Park, K.; Lim, Y. R.; Cha, E. H.; Park, J. $CoSe_2$ and $NiSe_2$ Nanocrystals as Superior Bifunctional Catalysts for Electrochemical and Photoelectrochemical Water Splitting. *ACS Appl. Mater. Interfaces* **2016**, *8*, 5327−5334.
(30) Yang, Y.; Xu, D.; Wu, Q.; Diao, P. Cu_2O/CuO Bilayered Composite as a High-Efficiency Photocathode for Photoelectrochemical Hydrogen Evolution Reaction. *Sci. Rep.* **2016**, *6*, 35158.
(31) Hou, C. C.; Fu, W. F.; Chen, Y. Self-Supported Cu-Based Nanowire Arrays as Noble-Metal-Free Electrocatalysts for Oxygen Evolution. *ChemSusChem* **2016**, *9*, 2069−2073.
(32) Riha, S. C.; Johnson, D. C.; Prieto, A. L. Cu_2Se Nanoparticles with Tunable Electronic Properties Due to a Controlled Solid-State Phase Transition Driven by Copper Oxidation and Cationic Conduction. *J. Am. Chem. Soc.* **2011**, *133*, 1383−1390.
(33) Xu, J.; Yang, Q.; Kang, W.; Huang, X.; Wu, C.; Wang, L.; Luo, L.; Zhang, W.; Lee, C. S. Water Evaporation Induced Conversion of CuSe Nanoflakes to Cu2−*x*Se Hierarchical Columnar Superstructures for High-Performance Solar Cell Applications. *Part. Part. Syst. Charact.* **2015**, *32*, 840−847.
(34) Liu, X.; Duan, X.; Peng, P.; Zheng, W. Hydrothermal synthesis of copper selenides with controllable phases and morphologies from an ionic liquid precursor. *Nanoscale* **2011**, *3*, 5090−5095.
(35) Lee, W.; Myung, N.; Rajeshwar, K.; Lee, C. W. Electrodeposition of Cu_2Se Semiconductor Thin Film on Se-Modified Polycrystalline Au Electrode. *J. Electrochem. Sci. Technol.* **2013**, *4*, 140−145.
(36) Liu, X.; Cui, S.; Sun, Z.; Ren, Y.; Zhang, X.; Du, P. Self-Supported Copper Oxide Electrocatalyst for Water Oxidation at Low Overpotential and Confirmation of Its Robustness by Cu K-Edge X-ray Absorption Spectroscopy. *J. Phys. Chem. C* **2016**, *120*, 831−840.
(37) Handoko, a. d.; Deng, S.; Deng, Y.; Cheng, A. W. F.; Chan, K. W.; Tan, H. R.; Pan, Y.; Tok, E. S.; Sow, C. H.; Yeo, B. S. Enhanced activity of H_2O_2-treated copper(II) oxide nanostructures for the electrochemical evolution of oxygen. *Catal. Sci. Technol.* **2016**, *6*, 269−274.
(38) Sun, W.; Song, Y.; Gong, X. Q.; Cao, L.; Yang, J. An efficiently tuned d-orbital occupation of IrO2 by doping with Cu for enhancing the oxygen evolution reaction activity. *Chem. Sci.* **2015**, *6*, 4993−4999.
(39) Serov, A.; Andersen, N. I.; Roy, A. J.; Matanovic, I.; Artyushkova, K.; Atanassov, P. $CuCo_2O_4$ ORR/OER Bi-Functional Catalyst: Influence of Synthetic Approach on Performance. *J. Electrochem. Soc.* **2015**, *162*, F449−F454.
(40) Hinogami, R.; Toyoda, K.; Aizawa, M.; Kawasaki, T.; Gyoten, H. Copper Delafossite Anode for Water Electrolysis. *ECS Trans.* **2013**, *58*, 27−31.
(41) Hou, C. C.; Chen, Q. Q.; Wang, C. J.; Liang, F.; Lin, Z.; Fu, W. F.; Chen, Y. Self-Supported Cedarlike Semimetallic Cu_3P Nanoarrays as a 3D High-Performance Janus Electrode for Both Oxygen and Hydrogen Evolution under Basic Conditions. *ACS Appl. Mater. Interfaces* **2016**, *8*, 23037−23048.
(42) Li, H.; Li, Q.; Wen, O.; Williams, T. B.; Adhikari, S.; Dun, C.; Lu, C.; Itanze, D.; Jiang, L.; Carroll, D. L.; Donati, G. L.; Lundin, P. M.; Qiu, Y.; Geyer, S. M. Colloidal Cobalt Phosphide Nanocrystals as Trifunctional Electrocatalysts for Overall Water Splitting Powered by a Zinc-Air Battery. *Adv. Mater.* **2018**, *30*, 1705796.
(43) Zhang, Z.; Ma, X.; Tang, J. (2018). Porous NiMoO 4− x/MoO 2 Hybrids as Highly Effective Electrocatalyst for Water Splitting Reaction. Journal of Materials Chemistry A. *J. Mater. Chem. A* **2018**, *6*, 12361.
(44) Li, C. W.; Kanan, M. W. CO_2 Reduction at Low Overpotential on Cu Electrodes Resulting from the Reduction of Thick Cu_2O Films. *J. Am. Chem. Soc.* **2012**, *134*, 7231−7234.
(45) Zhang, X.; Liu, J. X.; Zijlstra, B.; Filot, I. A. W.; Zhou, Z.; Sun, S.; Hensen, E. J. M. Optimum Cu nanoparticle catalysts for CO_2 hydrogenation towards methanol. *Nano Energy* **2018**, *43*, 200−209.
(46) Gawande, M. B.; Goswami, A.; Felpin, F. X.; Asefa, T.; Huang, X.; Silva, R.; Zou, X.; Zboril, R.; Varma, R. S. Cu and Cu-Based Nanoparticles: Synthesis and Applications in Catalysis. *Chem. Rev.* **2016**, *116*, 3722−3811.
(47) Shimkin, K. W.; Watson, D. A. Recent developments in copper-catalyzed radical alkylations of electron-rich π-systems. *Beilstein J. Org. Chem.* **2015**, *11*, 2278−2288.
(48) Van Den Berg, R.; Prieto, G.; Korpershoek, G.; van der Wal, L. I.; van Bunningen, A. J.; Lægsgaard-Jørgensen, S.; de Jongh, P. E.; de Jong, K. P. Structure sensitivity of Cu and CuZn catalysts relevant to industrial methanol synthesis. *Nat. Commun.* **2016**, *7*, 13057.
(49) Chemler, S. R. Copper's Contribution to Amination Catalysis. *Science* **2013**, *341*, 624−626.
(50) Yang, H.; Chen, Y.; Cui, X.; Wang, G.; Cen, Y.; Deng, T.; Yan, W.; Gao, J.; Zhu, S.; Olsbye, U.; Wang, J.; Fan, W. A Highly Stable Copper-Based Catalyst for Clarifying the Catalytic Roles of Cu^0 and Cu+ Species in Methanol Dehydrogenation. *Angew. Chem., Int. Ed.* **2018**, *57*, 1836−1840.
(51) Murray, R. M.; Heyding, R. D. The Copper−Selenium System at Temperatures to 850 K and Pressures To 50 Kbar. *Can. J. Chem.* **1975**, *53*, 878−887.

DOI: 10.1021/acsaem.8b00746
ACS Appl. Energy Mater. 2018, 1, 4075−4083